Bioconjugate Chemistry

pubs.acs.org/bc

Article

High-Affinity Points of Interaction on Antibody Allow Synthesis of Stable and Highly Functional Antibody−Gold Nanoparticle Conjugates

Samuel Okyem, Olatunde Awotunde, Tosin Ogunlusi, McKenzie B. Riley, and Jeremy D. Driskell*

Cite This: https://doi.org/10.1021/acs.bioconjchem.1c00261

Read Online

ACCESS | Metrics & More | Article Recommendations | Supporting Information

ABSTRACT: Many emerging nanobiotechnologies rely on the proper function of proteins immobilized on gold nanoparticles. Often, the surface chemistry of the AuNP is engineered to control the orientation, surface coverage, and structure of the adsorbed protein to maximize conjugate function. Here, we chemically modified antibody to investigate the effect of protein surface chemistries on adsorption to AuNPs. A monoclonal anti-horseradish peroxidase IgG antibody (anti-HRP) was reacted with N-succinimidyl acrylate (NSA) or reduced dithiobissuccinimidyl propionate (DSP) to modify lysine residues. Zeta potential measurements confirmed that both chemical modifications reduced the localized regions of positive charge on the protein surface, while the DSP modification incorporated additional free thiols. Dynamic light scattering confirmed that native and chemically modified antibodies adsorbed onto AuNPs to form bioconjugates; however, adsorption kinetics revealed that the NSA-modified antibody required significantly more time to allow for the formation of a hard corona. Moreover, conjugates formed with the NSA-modified antibody lost antigen-binding function, whereas unmodified and DSP-modified antibodies adsorbed onto AuNPs to form functional conjugates. These results indicate that high-affinity functional groups are required to prevent protein unfolding and loss of function when adsorbed on the AuNP surface. The reduced protein charge and high-affinity thiol groups on the DSP-modified antibody enabled pH-dependent control of protein orientation and the formation of highly active conjugates at solution pHs (<7.5) that are inaccessible with unmodified antibody due to conjugate aggregation. This study establishes parameters for protein modification to facilitate the formation of highly functional and stable protein−AuNP conjugates.

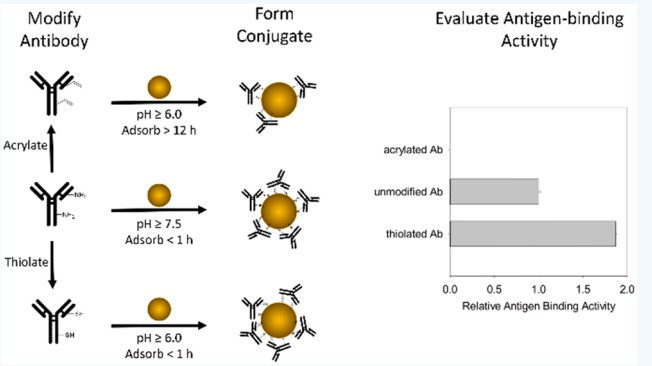

INTRODUCTION

Protein−gold nanoparticle conjugates are poised to play a critical role in next-generation biomedical technologies.[1−7] Advances in diagnostic testing,[8−15] tissue and cellular imaging,[16−18] photothermal therapy,[19] biocatalysis,[20] and drug delivery[21] have been achieved with the integration of functionalized gold nanoparticles. The overall success and widespread implementation of these nanoparticle-enabled technologies hinges on the effectiveness of the protein−nanoparticle conjugate, specifically the interfacial chemistry to immobilize the surface protein. The protein should retain its native conformation and confer an appropriate orientation to prevent a loss in activity upon immobilization.[22,23] Moreover, the attachment chemistry must be robust to prevent desorption in diverse and complex biological matrices. Thus, it is essential to understand the protein−AuNP interaction to control and maximize conjugate function.

To date, most biofunctionalization strategies have focused on surface modification of the AuNP as a first step to facilitate directed, robust binding of the protein without loss of function. For example, AuNPs can be carboxylated in a first step followed by EDC/NHS mediated coupling chemistry that targets the primary amine of lysine residues presented by proteins as a strategy to form a robust protein adlayer.[24−26] Surface modification of AuNPs to target oxidized carbohydrates on the Fc fragment of IgG antibodies has been explored as an effective means to modulate protein orientation.[27−29] AuNP functionalization with various ligands in combination with protein engineering to introduce site-specific protein modifications has been utilized to control protein orientation and provide high-affinity attachment to the AuNP surface, although this approach is not broadly applicable.[30−32] In other works, prefunctionalization of the AuNP surface was found to

Received: May 19, 2021
Revised: June 15, 2021

prevent protein denaturation upon binding to the AuNP surface.[33]

Herein, we explore an alternative approach to biofunctionalization, in which the protein is chemically modified as a first step followed by adsorption onto the AuNP surface. Interest in the formation of protein coronas around nanoparticles has led to a growing body of work dedicated to the interaction of proteins with AuNPs. Those works established that electrostatic interactions between the protein and the nanoparticle govern the stability and orientation[13,34−36] of the adsorbed protein and the number of S−Au interactions is largely responsible for the affinity of the protein−nanoparticle interaction.[31,37−40] For example, positively charged proteins can destabilize negatively charged nanoparticles to render the conjugate unstable via electrostatic bridging.[41−43] Moreover, solution pH modulates protein charge to directly impact the orientation of antibody adsorbed onto AuNPs, with preferred orientation adopted as the pH decreases.[34,35] However, when exploiting pH for directed orientation, there is a lower pH threshold at which the AuNPs aggregate. Capitalizing on these protein−AuNP interactions, Treuel et al. chemically modified bovine serum albumin (BSA) to modulate protein charge, thereby altering BSA orientation on the AuNP surface and leading to differences in cellular uptake of the bioconjugate.[36] Our group has previously demonstrated that acrylating the amino group on lysine residues reduces the overall protein charge to improve conjugate stability at low pH by circumventing electrostatic bridging of the AuNPs.[44,45] Lastly, antibodies have been modified with Traut's reagent to introduce additional thiols and increase the affinity of the protein−AuNP interaction.[46,47] Thus, these limited reports support the exploration of biofunctionalization with chemically modified proteins as a means to enhance conjugate stability and function.

In this work, we chemically modified an antibody to introduce high-affinity thiols or to reduce protein charge. We then studied the effect of these chemistries on the formation of a protein corona on AuNPs. First, the antibody was modified by reacting with N-succinimidyl acrylate (NSA) to neutralize positively charged lysine residues. This strategy extended the synthesis of stable antibody−AuNP conjugates to lower pHs, allowing further investigation into pH-controlled orientation. Second, antibody was modified by reacting with reduced dithiobissuccinimidyl propionate (DSP) to neutralize positively charged lysine residues and incorporate additional free thiol groups. This modification enabled the synthesis of stable conjugates at previously inaccessible low pHs and provided high-affinity moieties for the surface of AuNPs. The adsorption kinetics of the native and chemically modified antibodies were assessed using UV−vis spectrophotometry, dynamic light scattering, and zeta potential measurements. The fully formed conjugates were then compared with respect to antigen-binding activity. Moreover, solution pH was varied during antibody adsorption to investigate orientation effects. Our results revealed that functional groups with a propensity to adsorb onto AuNPs with high affinity are necessary to prevent protein unfolding. Additionally, we concluded that chemical modification of a protein is a viable approach to form highly stable and highly active bioconjugates. While this work focuses on IgG antibody adsorption, the physicochemical insight can be extended to other protein−AuNP systems.

RESULTS AND DISCUSSION

Antibody Chemical Modification and Characterization. Primary amines of lysine residues are protonated at physiological pH and are a significant source of positive surface charge on the protein. Thus, chemical modification of the surface accessible lysine residues, through an addition−elimination reaction, can mask the basic moiety and serve to modulate the protein charge. *In silico* analysis confirmed that acrylated lysine residues substantially reduce the positive charge on a fully characterized IgG.[45]

Antibody chemical modification was carried out experimentally using NSA and reduced DSP (referred to as DSP). We envisaged that acrolein and a thiol propionate group will be covalently bonded to primary amines of lysine residues upon reacting with NSA and reduced DSP, respectively (Scheme 1). The zeta potential of the unmodified, NSA-

Scheme 1. Modification of Lysine Side Chain to Acrylate (i) and Thiolate (ii) the Amino Group

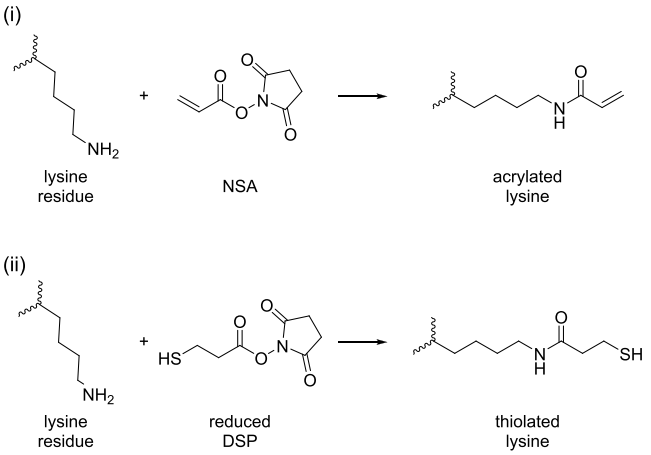

modified, and DSP-modified antibodies buffered at pH 7.5 was measured to assess protein charge and confirm chemical modification. The unmodified antibody exhibited a zeta potential of −10.5 ± 1.1 mV, whereas the NSA-modified Ab and DSP-modified Ab had zeta potentials of −22.7 ± 1.2 mV and −19.3 ± 2.6 mV, respectively (Figure 1A). Both modified antibodies presented a substantially more negative surface charge at pH 7.5 than the unmodified antibody as anticipated by the elimination of the basic characteristic of the lysine side chain. These data confirmed chemical modification of lysine residues through the primary amine and established that antibody surface charge can be manipulated via chemical modification.

Modification of the antibody with reduced DSP was further characterized by the quantitation of free thiols present on the unmodified and DSP-modified antibodies. The number of free thiols on the unmodified protein were quantified using Ellman's reagent and a previously established protocol (Figure 1B).[48,49] No free thiols were detected on the unmodified antibody, consistent with molecular models showing that each cysteine residue is involved in a disulfide bond and therefore not detected by Ellman's reagent.[37] However, 11 ± 3 free thiols were detected for the DSP-modified antibody. These results further confirmed chemical modification of the antibody and showed that free thiols can be added to proteins, which may impact adsorption to AuNPs.[46,47]

https://doi.org/10.1021/acs.bioconjchem.1c00261
Bioconjugate Chem. XXXX, XXX, XXX−XXX

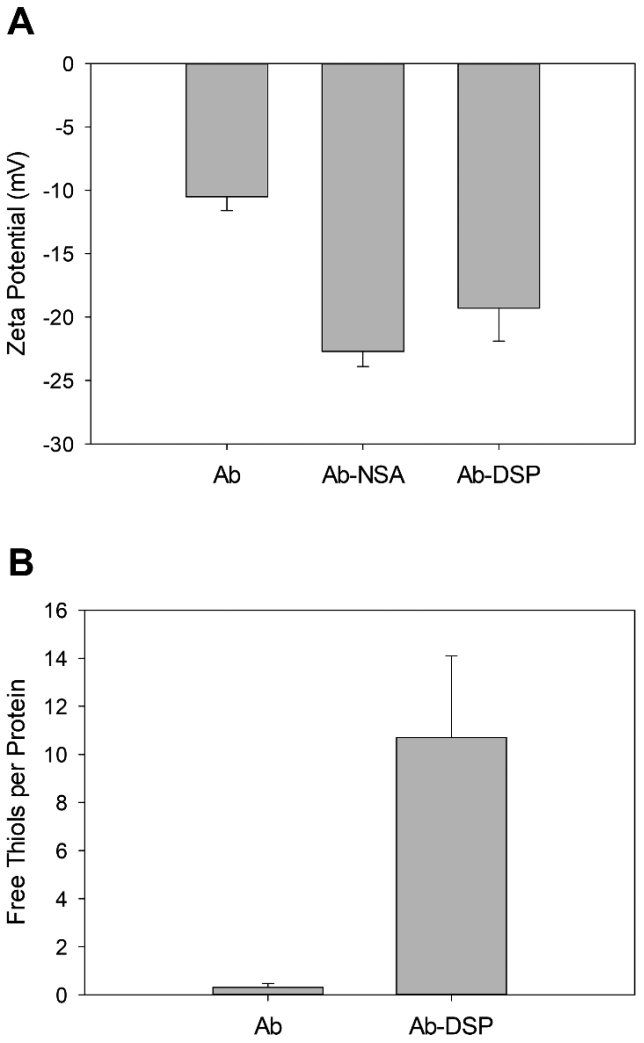

Figure 1. Zeta potential of unmodified, NSA-modified, and DSP-modified anti-HRP antibodies (A). Quantity of free thiols on unmodified and DSP-modified anti-HRP antibodies (B).

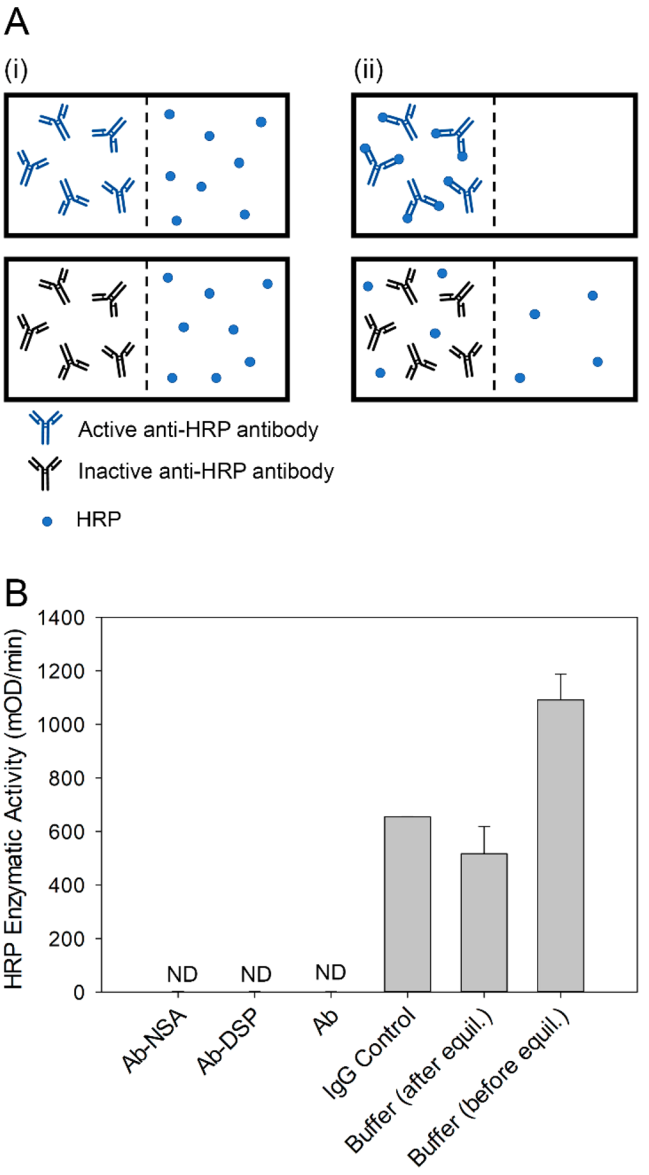

Figure 2. (A) Illustration of the equilibrium dialysis apparatus loaded with antibody sample in the left chamber and HRP in the right chamber (i) before and (ii) after equilibration. (B) Quantity of HRP remaining in the HRP chamber (right chamber) expressed as the enzymatic reaction rate. (ND = not detected; IgG Control = IgG2b isotype negative control; Buffer (after equil.) = signal in HRP chamber after equilibration with buffer; Buffer (before equil.) = signal in HRP chamber before equilibration).

Chemical modification of the antibody may affect the antigen binding site, consequently, resulting in the loss of function, i.e., the antigen binding capacity. Thus, equilibrium dialysis was performed to examine the antigen-binding activity of the anti-HRP antibodies free in solution before and after chemical modification. To this end, an HRP solution (10 nM) was added to one chamber of the dialysis device and an antibody solution (7 nM) was added to the adjacent sample chamber. The antibody solutions included unmodified anti-HRP antibody, NSA-modified anti-HRP antibody, and reduced DSP-modified anti-HRP antibody. A mouse IgG2b isotype control and buffer were also added to the sample chamber to serve as negative controls. The HRP and sample chambers were separated by a 100 kDa membrane, and the solutions were equilibrated for 3 h to allow HRP (MW 44 kDa) to equilibrate between the chambers, while the IgG was confined to its original chamber (MW 150 kDa) (Figure 2A). The concentrations of HRP and antibody were selected to allow the HRP molecules to be exhaustively captured by a functional antibody, given the divalency of an IgG antibody. After equilibration, the solution was removed from the chamber originally filled with HRP and the remaining HRP was measured based on enzymatic activity for the substrate ABTS.

Figures 2B and S1 show that no HRP was detected in the HRP chamber when equilibrated against a sample chamber filled with the unmodified, NSA-modified, or DSP-modified anti-HRP antibody. This result confirmed these antibodies bind the HRP antigen and completely extracted HRP from its original chamber. For the IgG isotype control and buffer, the HRP solution equilibrated to equimolar concentrations in both chambers (half the pre-equilibration concentration), since no binding occurred to concentrate the HRP in the sample chamber (Figures 2B and S1). The results established that NSA and DSP modification of the antibody did not diminish the antigen-binding function of the anti-HRP antibody. The antigen-binding function of the chemically modified anti-HRP

https://doi.org/10.1021/acs.bioconjchem.1c00261
Bioconjugate Chem. XXXX, XXX, XXX−XXX

antibodies was confirmed with an enzyme-linked immunosorbent assay (ELISA) (Supporting Information; Figure S2).

Kinetics of Hard and Soft Antibody Corona Formation on AuNPs. To evaluate the impact of chemical modification on the interaction between the antibody and AuNPs, an excess of unmodified, NSA-modified, and DSP-modified anti-HRP antibody was incubated with AuNPs for 1 h at pH 7.5 (antibody:AuNP = 4600:1). Previously, we determined that IgG antibodies spontaneously adsorb onto citrate-capped AuNP to provide a monolayer coverage within 1 h.[50] Excess unbound antibody was separated from the conjugates via centrifugation, and the purified conjugates were characterized using UV−vis spectrophotometry, dynamic light scattering (DLS), and zeta potential. Unconjugated 60 nm AuNPs exhibited an extinction maximum at 536 nm (Figure 3A). An extinction maximum was observed at 540−541 nm for the 60 nm AuNPs incubated with unmodified and DSP-modified antibody for 1 h (Figure 3A). This 4−5 nm red shift is characteristic of an adsorbed protein monolayer that causes a change in the conjugate refractive index.[51,52] Surprisingly, however, no shift in the extinction spectrum was observed for the 60 nm AuNPs incubated with the NSA-modified antibodies, and this result suggested that the NSA-modified antibody did not adsorb onto the AuNP within the 1 h incubation period.

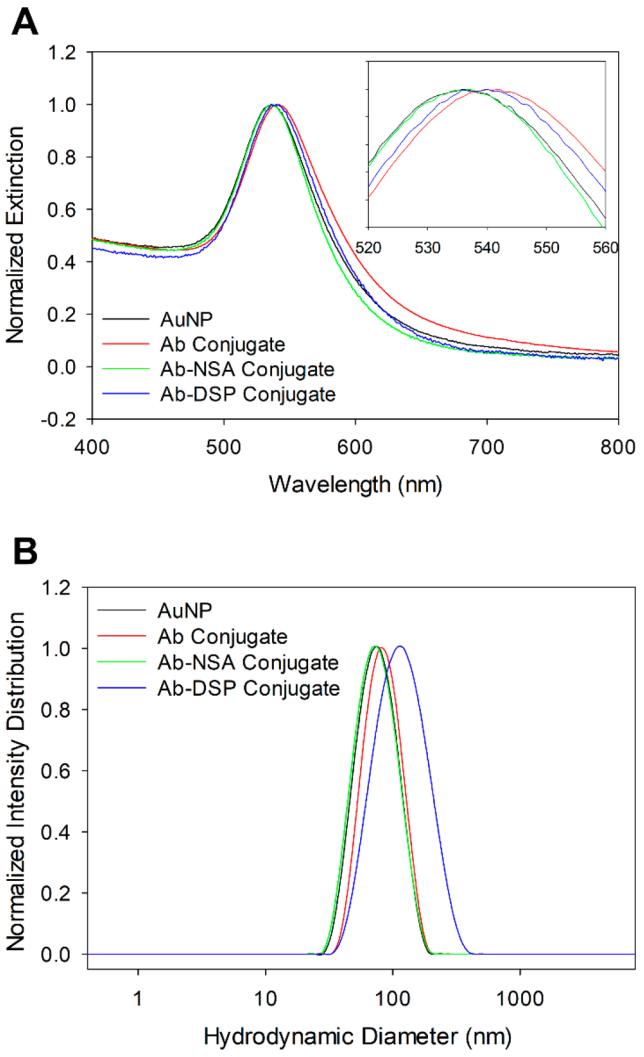

Figure 3. Extinction spectra (A) and DLS size distributions (B) of unconjugated AuNP and AuNP conjugates formed by incubation with unmodified Ab, Ab-NSA, and Ab-DSP after 1 h.

DLS analysis confirmed adsorption of unmodified and DSP-modified antibody on AuNPs after 1 h of incubation and purification, with mean hydrodynamic diameters of 75 ± 1 nm and 97 ± 2 nm, respectively (Figure 3B). The increase in hydrodynamic diameter from the adsorption of unmodified antibody indicated a monolayer formed, based on the size an IgG molecule and a measured hydrodynamic diameter of 62.3 ± 0.2 nm for the unconjugated AuNP. The DSP-modified antibody layer was slightly thicker than that of the unmodified antibody and implied different protein orientation, greater packing, or a bilayer of protein as a result of Ab-DSP dimerization via disulfide-mediated cross-linking. Interestingly, no significant change in AuNP size was detected for NSA-modified antibody AuNP conjugates (63.5 ± 0.4 nm) for the 1 h incubation time, further confirming the lack of conjugation.

Zeta potential measurements corroborated the UV−vis spectrophotometry and DLS size results. Unconjugated AuNPs possessed a zeta potential of −43 ± 3 mV due to the citrate adlayer formed during synthesis. Adsorption of the unmodified Ab and Ab-DSP increased the zeta potential to −32 ± 1 mV and −16 ± 1 mV, respectively, and these increases in zeta potential confirmed surface modification of the AuNP to form a bioconjugate. It was expected that the conjugate formed with the unmodified Ab would lead to a more positive zeta potential, considering the unmodified Ab was more positively charged than the Ab-DSP. Thus, we attributed this unanticipated result to greater loading of Ab-DSP or greater displacement of the citrate capping agent by the thiolated antibody. The zeta potential did not change for the AuNP incubated with Ab-NSA for 1 h (−44 ± 1 mV) relative to the unconjugated AuNP and confirmed that NSA modification of the antibody inhibited adsorption onto the AuNP.

To understand why there was no detectable adsorption of NSA-modified antibodies onto AuNPs after 1 h of incubation, we investigated the time evolution of the soft and hard antibody corona formed around the AuNPs, where the soft corona is composed of proteins that are loosely associated with the AuNP and the hard corona refers to the proteins that are strongly adsorbed onto the AuNP. Differentiation of the soft and hard corona is facilitated by centrifugation which removes the soft protein corona from the bioconjugate and leaves the hard corona intact.[53−56] Thus, AuNPs were incubated with Ab, Ab-NSA, or Ab-DSP for 1−24 h, and the conjugate size was measured via DLS before centrifugation to determine the combined thickness of the hard and soft corona. The conjugates were then centrifuged, the supernatant was discarded to remove the soft protein corona, and the conjugate size was evaluated to determine the thickness of the remaining hard protein corona. A soft corona of antibodies was observed within 1 h of incubation with AuNPs for the unmodified and both chemically modified antibodies (Figure 4A−C). The hydrodynamic diameter of the conjugate that included both the soft and hard corona ranged 89−97 nm, 89−99 nm, and 91−108 nm at all time points for the conjugates formed with Ab, Ab-NSA, and Ab-DSP, respectively, and no correlation was found between incubation time and the corona layer thickness. After centrifugation to remove the loosely bound proteins, a hard corona with similar thickness for each incubation time remained for conjugates formed from unmodified Ab and Ab-

https://doi.org/10.1021/acs.bioconjchem.1c00261
Bioconjugate Chem. XXXX, XXX, XXX−XXX

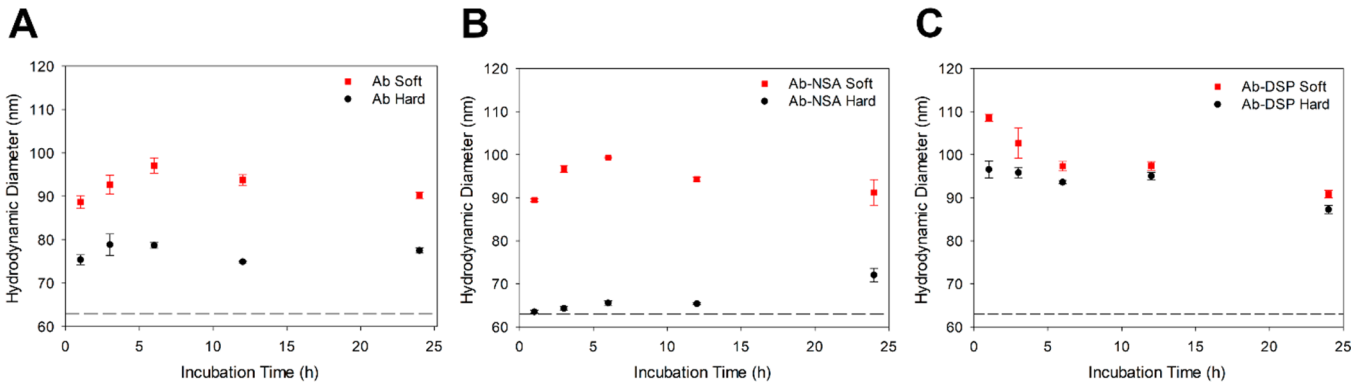

Figure 4. Kinetics of the formation of soft and hard protein corona on AuNP monitored by DLS for conjugates formed with unmodified Ab (A), Ab-NSA (B), and Ab-DSP (C). The dashed line represents the hydrodynamic diameter of the unconjugated AuNP (D_H = 62.3 nm).

DSP (Figure 4A and C). Notably, the hard corona thickness formed from the unmodified Ab is consistent with an IgG monolayer, while a slightly thicker hard layer is formed by Ab-DSP at each time point. In contrast, a hard corona was not formed with Ab-NSA within the first 12 h, and the size of the conjugate after centrifugation was equivalent to the size of unconjugated AuNP (Figure 4B). Zeta potential of purified conjugates confirms the rapid formation of hard antibody corona for unmodified Ab and Ab-DSP, whereas the adsorption of Ab-NSA slowly evolved over the 24 h incubation period (Figure 5).

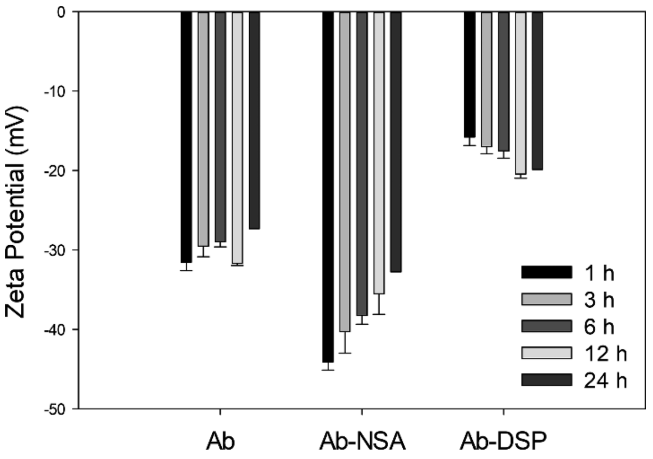

Figure 5. Kinetics of the hard corona formation monitored via zeta potential.

These results are supported by previous reports demonstrating that the long-range electrostatic attraction between localized positive regions on the antibodies and the negatively charged citrate-capped AuNP are responsible for the initial protein−AuNP interaction and facilitate the rapid formation of a soft corona.[13,30,32,34,36,44,57] Furthermore, the data demonstrated that the amount of positive surface charge remaining on both chemically modified Abs is sufficient to facilitate an electrostatic interaction for soft corona formation. Formation of a hard corona required moderate- to high-affinity interactions between the protein and AuNP, such as those provided by a free thiol presented by cysteine residues or an amine of a lysine residue.[66−68,21] Computational analysis of a fully characterized IgG2A (PDB ID 1IGT) similar to our antibody revealed all cysteine residues to be engaged in disulfide bonds; however, numerous solvent-accessible lysine residues were identified that are likely responsible for the strong interaction between the unmodified Ab and the AuNP to rapidly form a hard corona.[58−60] Likewise, the Ab-DSP converted ∼10 amino functional groups to free thiols which provided even greater affinity toward the AuNP to immediately form a hard corona upon adsorption. However, lysine residues were acrylated in the Ab-NSA to knock out high-affinity moieties for the AuNP present on the surface of the protein and replaced them with a low-affinity functional group. The formation of a hard corona by the Ab-NSA was only observed after 24 h of incubation. It has been previously reported that proteins undergo conformational changes and rearrangement upon interaction with AuNPs to maximize the binding affinity;[31,40,61,62] thus, it is likely that with extended incubation times, the Ab-NSA partially unfolded to expose lysine residues or disulfide bonds that cleaved in the presence of AuNP to form a hard corona.

Activity of Conjugates at Physiological pH (pH = 7.5). Antibody loading and orientation are critical to the antigen-binding capacity which directly affects the analytical performance of the bioconjugate in downstream applications.[29,63−68] Modulation of protein surface charge through chemical modifications[36,44] or pH[13,35] has been previously shown to impact both the loading density and orientation of protein upon adsorption onto AuNPs. Thus, we measured the antibody loading and antigen-binding capacity of bioconjugates formed with unmodified, NSA-modified, and DSP-modified anti-HRP antibody. To this end, antibody−AuNP conjugates were formed by allowing 24 h for the adsorption of unmodified Ab, Ab-NSA, or Ab-DSP at pH 7.5 to ensure formation of the hard corona. After centrifugation to remove excess antibody from the formed conjugates, the AuNP core was dissolved with KCN and the released antibody was quantified using the inherent fluorescence of the protein.[69] Figure 6A shows that 275 ± 45, 137 ± 4, and 301 ± 14 antibodies were adsorbed on each AuNP for conjugates formed with unmodified Ab, Ab-NSA, and Ab-DSP, respectively. The theoretical limit for antibody loading based on the physical size of an IgG molecules and the surface area of a 60 nm nanoparticle is ∼100−300 Ab/AuNP, depending on the orientation of the immobilized antibody.[35] Based on this estimate and previous work, the data confirmed that a monolayer of unmodified Ab and Ab-DSP was adsorbed onto the AuNP; however, the lower surface density of the Ab-NSA implied submonolayer formation, flat-on orientation of

https://doi.org/10.1021/acs.bioconjchem.1c00261
Bioconjugate Chem. XXXX, XXX, XXX−XXX

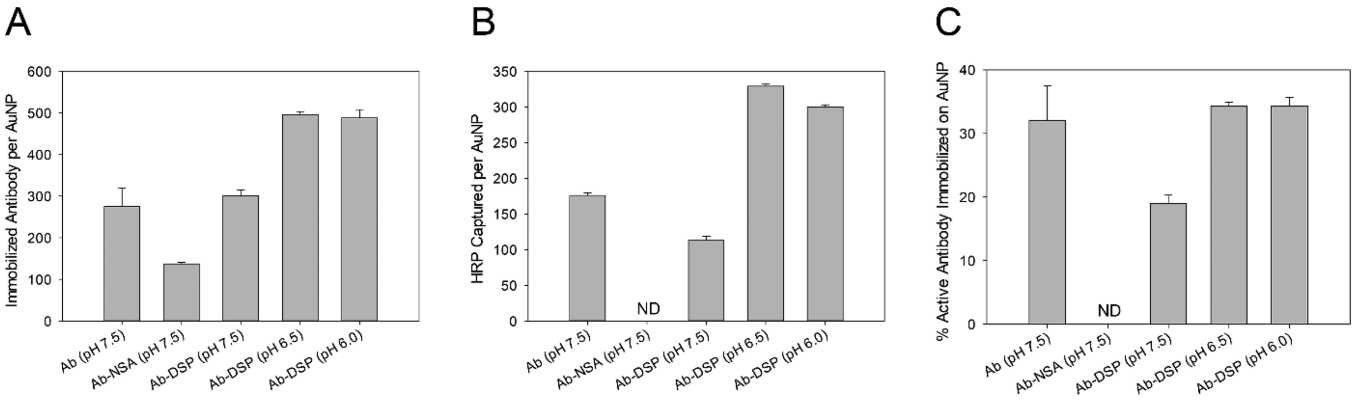

Figure 6. Antibody loading (A), maximum antigen binding capacity (B), and fraction of functional antibody immobilized on the AuNP conjugate (C) for conjugates formed with unmodified antibody at pH 7.5, NSA-modified antibody at pH 7.5, and DSP-modified antibody at pHs 7.5, 6.5, and 6.0. (ND = not detected).

the antibody, or unfolding of the Ab-NSA upon adsorption that increases its molecular footprint.

The maximum antigen binding capacity for the conjugates formed with unmodified Ab and Ab-DSP measured 176 ± 4 and 113 ± 6 antigen/conjugate, respectively, using an enzyme-mediated assay (Figure 6B).[70] Interestingly, the Ab-NSA conjugate did not bind antigen. Considering the antibody loading and antigen-binding capacity of each conjugate, the fraction of accessible and functional antigen-binding sites was calculated (Figure 6C). The adsorption of unmodified Ab resulted in 32% ± 5% of the F_{ab} sites with proper orientation and function, whereas the Ab-DSP resulted in 19% ± 6% of the F_{ab} sites with proper orientation and function. As demonstrated in Figure 2, neither NSA nor DSP modification of lysine hindered the antibody function when free in solution. Antibody loading was decreased to confirm that the antigen-binding activity was not influenced by steric hindrance, e.g., antibody overcrowding. The fraction of immobilized antibodies that maintain antigen-binding activity is similar for bioconjugates prepared with antibody loading at 50−100% of maximum loading capacity (Figure S3). The sensitivity of our protein assay prevented the quantitative analysis of bioconjugates with less than 50% antibody loading. Based on these results, we concluded that the decrease in antigen binding activity for the Ab-DSP was a result of unfavorable orientation. This conclusion is supported by previous work establishing that antibody charge governs orientation upon adsorption to AuNP and more positively charged protein (such as the unmodified Ab) confers an optimal orientation. We speculate that the Ab-NSA did not possess enough surface-accessible, high-affinity functional groups after acrylating the lysine residues, and the protein must unfold to adsorb onto the AuNP rendering it unable to bind antigen. This explanation is consistent with an increased incubation time to form a hard corona and reduced antibody loading on the Ab-NSA conjugate because of the larger footprint of an unfolded protein. Nevertheless, these results identify high-affinity functional groups as a requisite criterion to form functional protein−AuNP conjugates.

Impact of pH on Conjugate Formation and Activity. We have previously demonstrated that pH governs protein surface charge, thereby controlling the orientation of adsorbed antibody. Thus, we investigated the formation of Ab-AuNP conjugates formed with unmodified and DSP-modified antibody as a function of pH and the resulting antigen-binding capacity. Bioconjugates formed with NSA-modified antibodies were not explored, since they were found to be inactive upon adsorption onto AuNPs. AuNP suspensions were adjusted to pH 6.0, 6.5, or 7.5, and equivalent amounts of unmodified Ab or Ab-DSP were added to each suspension to evaluate the impact of pH on the interaction between the proteins and AuNPs. The AuNP suspension remained red after the addition of the unmodified Ab at pH 7.5; however, an immediate color change from red to purple was observed at pH 6.0 and 6.5, indicating protein-induced aggregation at the lower pHs. Extinction spectra were collected to confirm the formation of stable, monodisperse conjugates with unmodified Ab at pH 7.5 and the formation of large heterogeneous aggregates at pH 6.0 and 6.5 (Figure S4A). This pH-dependent aggregation was a result of electrostatic bridging between AuNPs that was mediated by the increased positive charge on the unmodified Ab at lower pH solutions.[44,45,71] In contrast, the AuNP suspensions remained red in color after the addition of Ab-DSP at each pH. Extinction spectra revealed equivalent red-shifted bands at each pH, relative to unconjugated AuNP, that signified monodisperse particles with an adsorbed protein layer (Figure S4B).[51,52] The DSP modification effectively reduced the number of localized positive regions on the antibody to mitigate electrostatic bridging and enabled the formation of stable conjugates over a broader pH range.

Antibody loading and antigen binding capacity for the Ab-DSP conjugates formed at pH 6.5 and 6.0 were quantified to evaluate the impact of pH. It is worth noting that conjugates prepared with unmodified antibody could not be analyzed at pH 6.5 or 6.0 since they aggregated at pH < 7.5; however, it was previously reported that antibody loading increases as the solution pH decreases for solution pH ranging from 8.5 to 7.5. At pH 6.5 and 6.0, the conjugates consisted of 496 ± 7 and 488 ± 20 Ab-DSP molecules per AuNP, respectively, compared to 301 ± 14 Ab-DSP/AuNP and 275 ± 45 Ab/AuNP at pH 7.5 (Figure 6A). The maximum antigen binding capacity was 329 ± 3 antigen/conjugate and 300 ± 3 antigen/conjugate for conjugates prepared at pH 6.5 and 6.0, respectively (Figure 6B). This represents an 87% and 70% increase in antigen binding capacity compared to the 176 ± 9 antigen/conjugate captured by the unmodified Ab at pH 7.5. However, when considering the increase in antibody loading at these lower pHs, the fraction of active Ab-DSP adsorbed on the AuNP was 34 ± 2% and 34 ± 4% at pH 6.5 and 6.0, respectively, equivalent to the faction of active antibody for

https://doi.org/10.1021/acs.bioconjchem.1c00261
Bioconjugate Chem. XXXX, XXX, XXX−XXX

unmodified antibody at pH 7.5 (Figure 6C). Thus, we concluded that the Ab-DSP did not confer an improved orientation on the AuNP at lower pH compared to the unmodified Ab at pH 7.5. More likely, the orientation of the unmodified Ab at pH 7.5 and DSP-modified Ab at pH 6.5 and 6.0 are similar, because these conditions lead to similar surface charges on the unmodified and DSP-modified antibodies since the DSP modification converts the basic lysine to a neutral side chain. Collectively, our results show that the antigen-binding performance of conjugates can be enhanced by modifying lysine residues to remove the positive charge, introducing a high-affinity functional group, and adsorbing the protein onto the AuNP at low pH; however, this improved performance is a result of greater Ab loading rather than a more favorable orientation.

CONCLUSIONS

We chemically modified surface-accessible lysine residues on an IgG anti-HRP antibody to reduce the protein surface charge, to block the protein amine groups that exhibit high affinity toward AuNP surfaces, and to increase the number of free thiols presented by the protein, and subsequently investigated the impact of these protein features on protein−AuNP interactions. Zeta potential measurements confirmed successful modification of the protein, and a functional assay using equilibrium dialysis established that the chemical modifications did not alter the antigen-binding function of the modified antibodies. DLS was used to measure the time-dependent evolution of the hard and soft corona formed around the AuNP. While each of the antibody variants quickly formed a soft corona, a hard corona was only formed in less than 24 h for proteins expressing high-affinity functional groups, e.g., primary amines and thiols. Acrylated lysine residues eliminated the high-affinity point of contact between the protein and the AuNP; thus, hard corona formation required unfolding of this protein to expose high-affinity moieties previously buried and inaccessible in the folded protein. Consequently, extended interaction times between this protein and the AuNP were required to form the hard corona and the adsorbed protein lost antigen binding function as a result of unfolding. Given the diversity of proteins and conflicting observations that have been reported regarding protein unfolding/folding and loss/gain of protein function upon adoption onto AuNPs, this work may provide valuable insight into those previous works. Thus, we have identified a strategy, chemical modification to introduce high-affinity functional groups, that will enable conjugation of proteins to nanoparticles without loss of function.

Thiolated lysine residues eliminated the positive charge yet replaced the high-affinity primary amine with a thiol which possesses even greater affinity for the AuNP surface. This modification enabled adsorption over an expanded pH range without suffering protein-induced AuNP aggregation. The resulting conjugate formed at pH 6.5 with DSP-modified antibody enhanced the antigen binding performance of the conjugate by 86% relative to the conjugate prepared with unmodified antibody that was limited to a minimum solution pH of 7.5. Thus, these results provide a pathway to synthesize highly active conjugates for enhanced analytical performance in biosensing applications and highly stable conjugates for *in vivo* applications in which nanoparticle aggregation is cause for health-related concerns.

EXPERIMENTAL METHODS

Materials. Citrate-capped gold nanoparticles with a nominal diameter of 60 nm (2.6×10^{10} AuNP/mL) were purchased from Ted Pella Inc. (Redding, CA) and employed in all studies. Mouse monoclonal anti-HRP IgG antibody (Clone 2H11) was obtained from My BioSource. One-step ABTS Substrate solution (2,2′-azinobis [3-ethylbenzothiazoline-6-sulfonic acid]-diammonium salt), horseradish peroxidase (HRP), and dithiobissuccinimidyl propionate (DSP) were purchased from Thermo Scientific (Rockford, IL). Phosphate buffers were prepared using anhydrous potassium phosphate dibasic and potassium phosphate monohydrate obtained from Mallinckrodt Chemicals, Inc. (Paris, KY) and Fischer Scientific (Fair Lawn, NJ), respectively. *N*-Succinimidyl acrylate (NSA) and Amicon ultra centrifugation filters (MWCO 100 kDa) were acquired from Sigma-Aldrich (St Louis, MO).

Chemical Modification and Characterization of Antibody. Anti-HRP antibody (Ab) was chemically modified using NSA and DSP. NSA (2 μL at 50 mM) was added to 50 μg of Ab. DSP was first reduced using TCEP resin according to the manufacture's protocol, and 2 μL of reduced DSP (50 mM) was added to 50 μg of Ab. The chemical modifier antibody solution reacted for 2 h at room temperature with gentle shaking. Excess unreacted chemical modifiers were removed with the use of an Amicon ultracentrifugation filter (MWCO 100 kDa). Glycerol was rinsed from the filter membrane with the addition of 500 μL of 2 mM phosphate buffer (pH 7.5) and centrifuged at 10 000 g for 5 min. The antibody chemical modifier reaction mixture was diluted to 500 μL and centrifuged at 14 000 g for 12 min. The filter was inverted and centrifuged at 1000 g for 3 min to recover the modified antibodies. The modified antibodies were quantified using a NanoDrop 2000C spectrophotometer (Thermo Scientific, Rockford, IL). Chemical modification was confirmed by measuring the zeta potential of the antibody before and after chemical modification using a Zetasizer Nano (Malvern Instruments). Moreover, DSP-modified Ab was further characterized by quantifying the addition of free thiols using Ellman's reagent and a previously reported procedure.[49]

Equilibrium dialysis and an HRP enzymatic assay were used to evaluate the antigen binding function of chemically modified antibodies. Fifty microliters of 1.0 μg/mL (6.7 nM) of unmodified Ab, NSA-modified Ab, DSP-modified Ab, or a mouse IgG isotype control was loaded into one chamber of the equilibrium dialysis apparatus (DispoEquilibrium Dialyzer; MWCO 100 kDa; Harvard Apparatus). The adjacent chamber was filled with 50 μL of 0.45 μg/mL (10.2 nM) of HRP and allowed to equilibrate for 3 h. After equilibration, 30 μL of solution from the chamber originally filled with HRP was withdrawn and mixed with 170 μL of 1-step ABTS solution. The enzymatic reaction rate was measured and directly correlated with the quantity of HRP remaining in the chamber.

Time-Dependent Formation of Soft and Hard Protein Corona on AuNPs. One hundred microliters of 60 nm AuNPs was pelleted by centrifuging at 5000 g for 5 min. The pelleted AuNPs were resuspended in 100 μL of 2 mM phosphate buffer at pH 7.5, unless stated otherwise. After pH adjustment of the AuNP suspension, 3 μg of antibody (chemically modified or unmodified) was added to the AuNPs and incubated for 1, 3, 6, 12, and 24 h. The size and zeta potential of the conjugates were measured *in situ*, i.e., without centrifugation to remove excess protein, to evaluate

https://doi.org/10.1021/acs.bioconjchem.1c00261
Bioconjugate Chem. XXXX, XXX, XXX−XXX

the formation of a soft protein corona at each time point. The conjugates were then centrifuged at 5000 g for 5 min, and the supernatant was discarded followed by resuspension of the pelleted AuNP conjugates in buffer. The centrifugation/resuspension cycle was carried out three times to ensure the removal of any nonadsorbed antibody or antibody present in the soft corona. The size and zeta potential of the purified antibody−AuNPs conjugates were measured at each time point to monitor the evolution of a hard protein corona.

Quantifying Antibody Immobilized onto AuNPs. A native protein fluorescence assay was used to quantify the number of proteins adsorbed onto AuNP.[69] Antibody−AuNP conjugates were purified to remove excess antibodies in solution by centrifuging at 5000 g for 5 min, carefully pipetting the clear supernatant from the pelleted conjugates, and resuspending the pelleted antibody−AuNPs in buffer. Three cycles of centrifugation/resuspension were carried out to ensure the removal of any nonadsorbed antibody. After the third centrifugation cycle, the supernatant was removed, and 10 μL of 100 mM potassium cyanide was added to the pelleted antibody−AuNP conjugates to digest the AuNP core and release antibodies into solution for protein quantification. The AuNP digestion was allowed to proceed for 2 h at room temperature, followed by the addition of 100 μL of 2 mM phosphate buffer (pH 7.5). Standard solutions of unmodified and chemically modified Ab (0−5 μg/mL) were prepared in a digested AuNP solution containing the same concentration of AuNP and KCN as in antibody−AuNP conjugates to match the matrix of the samples and standards. Florescence spectra of standards and conjugates were obtained using an excitation wavelength of 280 nm and an emission range of 320−350 nm. Florescence intensity in the range of 335−342 nm was integrated and used for antibody quantification.

The amount of AuNPs to which antibody is adsorbed was also determined using a PerkinElmer Optima 8300 inductively coupled plasma-optical emission spectrometer (ICP-OES). Fifty microliters of digested antibody−AuNP conjugates used for the antibody florescence assay was diluted to 5 mL with 2% nitric acid. Standard solutions of gold (0.1−1 mg/L) were prepared in 2% nitric acid. The number of AuNPs was calculated by dividing the mass of gold in the conjugate samples extrapolated from ICP-OES calibration curve by the mass of a 60 nm AuNP (2.18×10^{-15} g).

Quantifying Antigen Binding Sites on Conjugates. The antigen binding activity of antibodies adsorbed onto AuNPs was determined by a previously described HRP enzymatic assay.[70] Briefly, 100 μL of purified antibody−AuNP conjugate was incubated with 3 μg of HRP for 1 h to saturate all available and functional binding sites presented by the conjugates. Excess unbound HRP was removed by three centrifuge/wash cycles at 5000 g for 5 min. Standard solutions of HRP (0.1−0.7 μg/mL) were prepared to generate a calibration curve and used to quantify the amount of HRP captured by conjugates. A 10 μL aliquot of standards and conjugates was mixed with 1-step ABTS solution, and the enzymatic rate was determined by measuring the absorbance of the oxidized product at 415 nm for 20 min at 10 s intervals using a Bio-Rad microplate plate reader. To correlate the number of HRP molecules captured to the number of antibodies per AuNP, the number of AuNPs present in the 100 μL antibody−AuNP conjugate suspension used for the HRP assay was determined using ICP-OES as described above.

Instrumentation. *Dynamic Light Scattering (DLS) and Zeta Potential Measurement.* Hydrodynamic diameter and zeta potential of unmodified antibody, chemically modified antibodies, and antibody−AuNP conjugates were measured using a Zetasizer Nano ZSP (Malvern Instruments) equipped with noninvasive back scatter optics. Antibodies were filtered with a 0.02 μm filter prior to DLS analysis. A folded capillary cuvette was filled with filtered buffer, and a 20 μL aliquot of antibodies or conjugates was carefully introduced to the bottom of the cuvette using the diffusion barrier technique. Hydrodynamic diameter and zeta potential were measured in triplicate. Fifteen runs were averaged for each measurement. A built-in Smoluchowksi method for aqueous media was adopted for all DLS measurement, and the Z-average was reported as the hydrodynamic diameter.

UV−vis Measurement. A Cary 1 Bio UV−vis dual-beam spectrophotometer was used to obtain extinction spectra of protein−AuNP conjugates. The spectra were collected over a range of 350−900 at 0.5 nm increments with a spectral bandwidth of 0.1 nm. HRP enzymatic assay absorbance was collected using an iMark Bio-Rad high throughput microplate reader. Enzyme kinetics were monitored at 415 nm for 20 min at 10 s intervals.

■ ASSOCIATED CONTENT

Supporting Information

The Supporting Information is available free of charge at https://pubs.acs.org/doi/10.1021/acs.bioconjchem.1c00261.

Kinetics plot for equilibrium dialysis (Figure S1), ELISA procedure for antibody activity, ELISA results for antibody activity (Figure S2), Antibody loading, antigen binding capacity and antibody activity for bioconjugates as a function of antibody loading (Figure S3), Extinction spectra of conjugates as a function of pH (Figure S4) (PDF)

■ AUTHOR INFORMATION

Corresponding Author

Jeremy D. Driskell − *Department of Chemistry, Illinois State University, Normal, Illinois 61790, United States;* orcid.org/0000-0001-5082-898X; Email: jdriske@ilstu.edu

Authors

Samuel Okyem − *Department of Chemistry, Illinois State University, Normal, Illinois 61790, United States*

Olatunde Awotunde − *Department of Chemistry, Illinois State University, Normal, Illinois 61790, United States*

Tosin Ogunlusi − *Department of Chemistry, Illinois State University, Normal, Illinois 61790, United States*

McKenzie B. Riley − *Department of Chemistry, Illinois State University, Normal, Illinois 61790, United States*

Complete contact information is available at: https://pubs.acs.org/10.1021/acs.bioconjchem.1c00261

Notes

The authors declare no competing financial interest.

■ ACKNOWLEDGMENTS

This work was funded by the National Science Foundation through the Macromolecular, Supramolecular and Nanochemistry Program, Award # CHE-1807126. O.A. and S.O.

would like to thank the Illinois State University Department of Chemistry for partial support.

REFERENCES

(1) Das, M., Shim, K. H., An, S. S. A., and Yi, D. K. (2011) Review on gold nanoparticles and their applications. *Toxicol. Env. Health Sci. 3*, 193−205.
(2) Dreaden, E. C., Alkilany, A. M., Huang, X., Murphy, C. J., and El-Sayed, M. A. (2012) The golden age: gold nanoparticles for biomedicine. *Chem. Soc. Rev. 41*, 2740−2779.
(3) Dykman, L., and Khlebtsov, N. (2012) Gold nanoparticles in biomedical applications: recent advances and perspectives. *Chem. Soc. Rev. 41*, 2256−2282.
(4) Giljohann, D. A., Seferos, D. S., Daniel, W. L., Massich, M. D., Patel, P. C., and Mirkin, C. A. (2010) Gold Nanoparticles for Biology and Medicine. *Angew. Chem., Int. Ed. 49*, 3280−3294.
(5) Li, Y., and Lee, J.-S. (2020) Insights into Characterization Methods and Biomedical Applications of Nanoparticle-Protein Corona. *Materials 13*, 3093.
(6) Yang, X., Yang, M. X., Pang, B., Vara, M., and Xia, Y. N. (2015) Gold Nanomaterials at Work in Biomedicine. *Chem. Rev. 115*, 10410−10488.
(7) Yeh, Y.-C., Creran, B., and Rotello, V. M. (2012) Gold nanoparticles: preparation, properties, and applications in bionanotechnology. *Nanoscale 4*, 1871−1880.
(8) Frimpong, R., Jang, W., Kim, J.-H., and Driskell, J. D. (2021) Rapid vertical flow immunoassay on AuNP plasmonic paper for SERS-based point of need diagnostics. *Talanta 223*, 121739.
(9) Zhou, W., Gao, X., Liu, D., and Chen, X. (2015) Gold Nanoparticles for In Vitro Diagnostics. *Chem. Rev. 115*, 10575−10636.
(10) Granger, J. H., Schlotter, N. E., Crawford, A. C., and Porter, M. D. (2016) Prospects for point-of-care pathogen diagnostics using surface-enhanced Raman scattering (SERS). *Chem. Soc. Rev. 45*, 3865−3882.
(11) Jans, H., and Huo, Q. (2012) Gold nanoparticle-enabled biological and chemical detection and analysis. *Chem. Soc. Rev. 41*, 2849−2866.
(12) Lopez, A., Lovato, F., Hwan Oh, S., Lai, Y. H., Filbrun, S., Driskell, E. A., and Driskell, J. D. (2016) SERS immunoassay based on the capture and concentration of antigen-assembled gold nanoparticles. *Talanta 146*, 388−393.
(13) Parolo, C., de la Escosura-Muñiz, A., Polo, E., Grazú, V., de la Fuente, J. M., and Merkoçi, A. (2013) Design, Preparation, and Evaluation of a Fixed-Orientation Antibody/Gold-Nanoparticle Conjugate as an Immunosensing Label. *ACS Appl. Mater. Interfaces 5*, 10753−10759.
(14) Penn, M. A., Drake, D. M., and Driskell, J. D. (2013) Accelerated Surface-Enhanced Raman Spectroscopy (SERS)-Based Immunoassay on a Gold-Plated Membrane. *Anal. Chem. 85*, 8609−8617.
(15) Saha, K., Agasti, S. S., Kim, C., Li, X., and Rotello, V. M. (2012) Gold Nanoparticles in Chemical and Biological Sensing. *Chem. Rev. 112*, 2739−2779.
(16) Li, W., and Chen, X. (2015) Gold nanoparticles for photoacoustic imaging. *Nanomedicine 10*, 299−320.
(17) Murphy, C. J., Gole, A. M., Stone, J. W., Sisco, P. N., Alkilany, A. M., Goldsmith, E. C., and Baxter, S. C. (2008) Gold Nanoparticles in Biology: Beyond Toxicity to Cellular Imaging. *Acc. Chem. Res. 41*, 1721−1730.
(18) Xiao, T., Qin, J., Peng, C., Guo, R., Lu, X., and Shi, X. (2020) A Dendrimer-Based Dual Radiodense Element-Containing Nanoplatform for Targeted Enhanced Tumor Computed Tomography Imaging. *Langmuir 36*, 3096−3103.
(19) Ali, M. R. K., Wu, Y., and El-Sayed, M. A. (2019) Gold-Nanoparticle-Assisted Plasmonic Photothermal Therapy Advances Toward Clinical Application. *J. Phys. Chem. C 123*, 15375−15393.
(20) Díaz, S. A., Choo, P., Oh, E., Susumu, K., Klein, W. P., Walper, S. A., Hastman, D. A., Odom, T. W., and Medintz, I. L. (2021) Gold Nanoparticle Templating Increases the Catalytic Rate of an Amylase, Maltase, and Glucokinase Multienzyme Cascade through Substrate Channeling Independent of Surface Curvature. *ACS Catal. 11*, 627−638.
(21) Ghosh, P., Han, G., De, M., Kim, C. K., and Rotello, V. M. (2008) Gold nanoparticles in delivery applications. *Adv. Drug Delivery Rev. 60*, 1307−1315.
(22) Hong, R., Fischer, N. O., Verma, A., Goodman, C. M., Emrick, T., and Rotello, V. M. (2004) Control of Protein Structure and Function through Surface Recognition by Tailored Nanoparticle Scaffolds. *J. Am. Chem. Soc. 126*, 739−743.
(23) Mangini, V., Maggi, V., Trianni, A., Melle, F., De Luca, E., Pennetta, A., Del Sole, R., Ventura, G., Cataldi, T. R. I., and Fiammengo, R. (2020) Directional Immobilization of Proteins on Gold Nanoparticles Is Essential for Their Biological Activity: Leptin as a Case Study. *Bioconjugate Chem. 31*, 74−81.
(24) Jazayeri, M. H., Amani, H., Pourfatollah, A. A., Pazoki-Toroudi, H., and Moghadam, B. S. (2016) Various methods of gold nanoparticles (GNPs) conjugation to antibodies. *Sens. Biosens. Res. 9*, 17−22.
(25) Raghav, R., and Srivastava, S. (2016) Immobilization strategy for enhancing sensitivity of immunosensors: L-Asparagine-AuNPs as a promising alternative of EDC-NHS activated citrate-AuNPs for antibody immobilization. *Biosens. Bioelectron. 78*, 396−403.
(26) Yan, Q., Zheng, H.-N., Jiang, C., Li, K., and Xiao, S.-J. (2015) EDC/NHS activation mechanism of polymethacrylic acid: anhydride versus NHS-ester. *RSC Adv. 5*, 69939−69947.
(27) Duval, F., van Beek, T. A., and Zuilhof, H. (2015) Key steps towards the oriented immobilization of antibodies using boronic acids. *Analyst 140*, 6467−6472.
(28) Kumar, S., Aaron, J., and Sokolov, K. (2008) Directional conjugation of antibodies to nanoparticles for synthesis of multiplexed optical contrast agents with both delivery and targeting moieties. *Nat. Protoc. 3*, 314−320.
(29) Lin, P. C., Chen, S. H., Wang, K. Y., Chen, M. L., Adak, A. K., Hwu, J. R. R., Chen, Y. J., and Lin, C. C. (2009) Fabrication of Oriented Antibody-Conjugated Magnetic Nanoprobes and Their Immunoaffinity Application. *Anal. Chem. 81*, 8774−8782.
(30) Lin, W., Insley, T., Tuttle, M. D., Zhu, L., Berthold, D. A., Král, P., Rienstra, C. M., and Murphy, C. J. (2015) Control of Protein Orientation on Gold Nanoparticles. *J. Phys. Chem. C 119*, 21035−21043.
(31) Siriwardana, K., Wang, A., Vangala, K., Fitzkee, N., and Zhang, D. (2013) Probing the Effects of Cysteine Residues on Protein Adsorption onto Gold Nanoparticles Using Wild-Type and Mutated GB3 Proteins. *Langmuir 29*, 10990−10996.
(32) Wang, A., Perera, Y. R., Davidson, M. B., and Fitzkee, N. C. (2016) Electrostatic Interactions and Protein Competition Reveal a Dynamic Surface in Gold Nanoparticle-Protein Adsorption. *J. Phys. Chem. C 120*, 24231−24239.
(33) Moyano, D. F., and Rotello, V. M. (2011) Nano Meets Biology: Structure and Function at the Nanoparticle Interface. *Langmuir 27*, 10376−10385.
(34) Puertas, S., Batalla, P., Moros, M., Polo, E., del Pino, P., Guisán, J. M., Grazú, V., and de la Fuente, J. M. (2011) Taking Advantage of Unspecific Interactions to Produce Highly Active Magnetic Nanoparticle-Antibody Conjugates. *ACS Nano 5*, 4521−4528.
(35) Ruiz, G., Tripathi, K., Okyem, S., and Driskell, J. D. (2019) pH Impacts the Orientation of Antibody Adsorbed onto Gold Nanoparticles. *Bioconjugate Chem. 30*, 1182−1191.
(36) Treuel, L., Brandholt, S., Maffre, P., Wiegele, S., Shang, L., and Nienhaus, G. U. (2014) Impact of Protein Modification on the Protein Corona on Nanoparticles and Nanoparticle-Cell Interactions. *ACS Nano 8*, 503−513.
(37) Awotunde, O., Okyem, S., Chikoti, R., and Driskell, J. D. (2020) Role of Free Thiol on Protein Adsorption to Gold Nanoparticles. *Langmuir 36*, 9241−9249.

https://doi.org/10.1021/acs.bioconjchem.1c00261
Bioconjugate Chem. XXXX, XXX, XXX−XXX

(38) Siriwardana, K., LaCour, A., and Zhang, D. (2016) Critical Sequence Dependence in Multicomponent Ligand Binding to Gold Nanoparticles. *J. Phys. Chem. C 120*, 6900−6905.
(39) Vangala, K., Ameer, F., Salomon, G., Le, V., Lewis, E., Yu, L. Y., Liu, D., and Zhang, D. M. (2012) Studying Protein and Gold Nanoparticle Interaction Using Organothiols as Molecular Probes. *J. Phys. Chem. C 116*, 3645−3652.
(40) Wang, A., Vangala, K., Vo, T., Zhang, D., and Fitzkee, N. C. (2014) A Three-Step Model for Protein-Gold Nanoparticle Adsorption. *J. Phys. Chem. C 118*, 8134−8142.
(41) Bharti, B., Meissner, J., and Findenegg, G. H. (2011) Aggregation of Silica Nanoparticles Directed by Adsorption of Lysozyme. *Langmuir 27*, 9823−9833.
(42) Bharti, B., Meissner, J., Klapp, S. H. L., and Findenegg, G. H. (2014) Bridging interactions of proteins with silica nanoparticles: The influence of pH, ionic strength and protein concentration. *Soft Matter 10*, 718−728.
(43) Neupane, S., Pan, Y., Takalkar, S., Bentz, K., Farmakes, J., Xu, Y., Chen, B., Liu, G., Qian, S. Y., and Yang, Z. (2017) Probing the Aggregation Mechanism of Gold Nanoparticles Triggered by a Globular Protein. *J. Phys. Chem. C 121*, 1377−1386.
(44) Filbrun, S. L., Mandl, A., Lovato, F., Oh, S. H., Driskell, E. A., and Driskell, J. D. (2017) Chemical Modification of Antibody Enables the Formation of Stable Antibody-Gold Nanoparticle Conjugates for Biosensing. *Analyst 142*, 4456.
(45) Okyem, S., Awotunde, O., Ogunlusi, T., Riley, M. B., and Driskell, J. D. (2021) Probing the Mechanism of Antibody-Triggered Aggregation of Gold Nanoparticles. *Langmuir 37*, 2993.
(46) Wang, X. F., Mei, Z., Wang, Y. Y., and Tang, L. (2015) Gold nanorod biochip functionalization by antibody thiolation. *Talanta 136*, 1−8.
(47) Wang, X. F., Mei, Z., Wang, Y. Y., and Tang, L. (2017) Comparison of four methods for the biofunctionalization of gold nanorods by the introduction of sulfhydryl groups to antibodies. *Beilstein J. Nanotechnol. 8*, 372−380.
(48) Badyal, J. P., Cameron, A. M., Cameron, N. R., Coe, D. M., Cox, R., Davis, B. G., Oates, L. J., Oye, G., and Steel, P. G. (2001) A simple method for the quantitative analysis of resin bound thiol groups. *Tetrahedron Lett. 42*, 8531−8533.
(49) Ellman, G. L. (1959) Tissue sulfhydryl groups. *Arch. Biochem. Biophys. 82*, 70−77.
(50) James, A. E., and Driskell, J. D. (2013) Monitoring gold nanoparticle conjugation and analysis of biomolecular binding with nanoparticle tracking analysis (NTA) and dynamic light scattering (DLS). *Analyst 138*, 1212−1218.
(51) Khlebtsov, N. G., Bogatyrev, V. A., Dykman, L. A., and Melnikov, A. G. (1996) Spectral Extinction of Colloidal Gold and Its Biospecific Conjugates. *J. Colloid Interface Sci. 180*, 436−445.
(52) Pollitt, M. J., Buckton, G., Piper, R., and Brocchini, S. (2015) Measuring antibody coatings on gold nanoparticles by optical spectroscopy. *RSC Adv. 5*, 24521−24527.
(53) Baimanov, D., Cai, R., and Chen, C. Y. (2019) Understanding the Chemical Nature of Nanoparticle-Protein Interactions. *Bioconjugate Chem. 30*, 1923−1937.
(54) Giri, K., Shameer, K., Zimmermann, M. T., Saha, S., Chakraborty, P. K., Sharma, A., Arvizo, R. R., Madden, B. J., Mccormick, D. J., Kocher, J. P. A., et al. (2014) Understanding Protein-Nanoparticle Interaction: A New Gateway to Disease Therapeutics. *Bioconjugate Chem. 25*, 1078−1090.
(55) Vilanova, O., Mittag, J. J., Kelly, P. M., Milani, S., Dawson, K. A., Radler, J. O., and Franzese, G. (2016) Understanding the Kinetics of Protein-Nanoparticle Corona Formation. *ACS Nano 10*, 10842−10850.
(56) Yadav, I., Kumar, S., Aswal, V. K., and Kohlbrecher, J. (2017) Structure and Interaction in the pH-Dependent Phase Behavior of Nanoparticle-Protein Systems. *Langmuir 33*, 1227−1238.
(57) Brewer, S. H., Glomm, W. R., Johnson, M. C., Knag, M. K., and Franzen, S. (2005) Probing BSA Binding to Citrate-Coated Gold Nanoparticles and Surfaces. *Langmuir 21*, 9303−9307.
(58) Harris, L. J., Larson, S. B., Hasel, K. W., and McPherson, A. (1997) Refined Structure of an Intact IgG2a Monoclonal Antibody. *Biochemistry 36*, 1581−1597.
(59) Pettersen, E. F., Goddard, T. D., Huang, C. C., Couch, G. S., Breenblatt, D. M., Meng, E. C., and Ferrin, T. E. (2004) UCSF Chimera–a Visualization System for Exploratory Research and Analysis. *J. Comput. Chem. 25*, 1605−1612.
(60) Porollo, A. A., Adamczak, R., and Meller, J. (2004) POLYVIEW: a flexible visualization tool for structural and functional annotations of proteins. *Bioinformatics 20*, 2460−2462.
(61) Goy-Lopez, S., Juarez, J., Alatorre-Meda, M., Casals, E., Puntes, V. F., Taboada, P., and Mosquera, V. (2012) Physicochemical Characteristics of Protein-NP Bioconjugates: The Role of Particle Curvature and Solution Conditions on Human Serum Albumin Conformation and Fibrillogenesis Inhibition. *Langmuir 28*, 9113−9126.
(62) Milani, S., Bombelli, F. B., Pitek, A. S., Dawson, K. A., and Radler, J. (2012) Reversible versus Irreversible Binding of Transferrin to Polystyrene Nanoparticles: Soft and Hard Corona. *ACS Nano 6*, 2532−2541.
(63) Joshi, P. P., Yoon, S. J., Hardin, W. G., Emelianov, S., and Sokolov, K. V. (2013) Conjugation of Antibodies to Gold Nanorods through Fc Portion: Synthesis and Molecular Specific Imaging. *Bioconjugate Chem. 24*, 878−888.
(64) Kausaite-Minkstimiene, A., Ramanaviciene, A., Kirlyte, J., and Ramanavicius, A. (2010) Comparative Study of Random and Oriented Antibody Immobilization Techniques on the Binding Capacity of Immunosensor. *Anal. Chem. 82*, 6401−6408.
(65) Puertas, S., Moros, M., Fernandez-Pacheco, R., Ibarra, M. R., Grazu, V., and de la Fuente, J. M. (2010) Designing novel nano-immunoassays: antibody orientation versus sensitivity. *J. Phys. D: Appl. Phys. 43*, 474012.
(66) Saha, B., Evers, T. H., and Prins, M. W. J. (2014) How Antibody Surface Coverage on Nanoparticles Determines the Activity and Kinetics of Antigen Capturing for Biosensing. *Anal. Chem. 86*, 8158−8166.
(67) Saha, B., Songe, P., Evers, T. H., and Prins, M. W. J. (2017) The influence of covalent immobilization conditions on antibody accessibility on nanoparticles. *Analyst 142*, 4247−4256.
(68) Song, H. Y., Zhou, X. D., Hobley, J., and Su, X. D. (2012) Comparative Study of Random and Oriented Antibody Immobilization as Measured by Dual Polarization Interferometry and Surface Plasnnon Resonance Spectroscopy. *Langmuir 28*, 997−1004.
(69) Kozlowski, R., Ragupathi, A., and Dyer, R. B. (2018) Characterizing the Surface Coverage of Protein-Gold Nanoparticle Bioconjugates. *Bioconjugate Chem. 29*, 2691−2700.
(70) Tripathi, K., and Driskell, J. D. (2018) Quantifying Bound and Active Antibodies Conjugated to Gold Nanoparticles: A Comprehensive and Robust Approach To Evaluate Immobilization Chemistry. *ACS Omega 3*, 8253−8259.
(71) Neupane, S., Pan, Y., Li, H., Patnode, K., Farmakes, J., Liu, G., and Yang, Z. (2018) Engineering Protein-Gold Nanoparticle/Nanorod Complexation via Surface Modification for Protein Immobilization and Potential Therapeutic Applications. *ACS Appl. Nano Mater. 1*, 4053−4063.

https://doi.org/10.1021/acs.bioconjchem.1c00261
Bioconjugate Chem. XXXX, XXX, XXX−XXX